

## RADIAL-LONGITUDINAL COUPLING IN CYCLOTRONS AND FOCUSING COMPLEMENTARITY\*

M. M. GORDON and FELIX MARTI

*Cyclotron Laboratory, Michigan State University, East Lansing, Michigan 48824 USA*

*(Received August 6, 1981; in final form October 21, 1981)*

The coupling of radial and longitudinal motion in cyclotrons is reconsidered, and following Schulte and Hagedoorn, the definition of the phase  $\phi$  is revised so as to make it a constant of the motion for a monoenergetic group of ions executing radial oscillations. This revision helps to preserve energy homogeneity for the group, and also provides a simpler evaluation of the inertial force acting on the radial oscillations as a result of the outward shift of the equilibrium orbit at each gap crossing. This force is shown to produce what might be called "radial electric focusing" since it strongly resembles, and is actually complementary to, the well-known vertical electric focusing. That is, acceleration conditions which increase the vertical focusing will simultaneously decrease the radial focusing to a comparable extent. The resultant change in  $\nu_r$  is evaluated for a fairly general *dee* geometry, and the conditions for radial instability near  $\nu_r = 1$  are then discussed. These results are applied to a variety of cyclotrons including one at Indiana and the TRIUMF machine. In the latter case, some detailed calculations are presented to demonstrate how well the simple theory works when the acceleration is strongly non-adiabatic, but the motion is still linear.

### 1. INTRODUCTION

For most cyclic accelerators, the fractional energy gain per turn is so small that the acceleration process can be accurately described as "adiabatic". The most common exceptions to this rule are cyclotrons with fixed frequency rf systems since these machines accelerate ions for relatively small numbers of turns starting, in most cases, from nearly zero energy.

As a result, the median plane motion in cyclotrons is accompanied by an unusually strong coupling between the acceleration process and the radial oscillations within the beam. The strength of this coupling varies inversely with turn number, so that its effects are most pronounced in the central region. In many cases, however, these effects remain significant throughout the cyclotron. This is especially true when the rf system operates on a high harmonic of the orbital frequency since the coupling strength is also proportional to the harmonic number.

Certain aspects of the coupling process have been known for a long time, but the analytical treatments have all been rather specialized. There is, for example, the effect of a voltage asymmetry in classical cyclotrons, which was analyzed by Cohen.<sup>1</sup> In addition, there are the

"electric gap crossing resonance" phenomena associated with the use of one or two dees in cyclotrons with three sector magnets.<sup>2</sup>

More recently, Schulte and Hagedoorn<sup>3</sup> have undertaken the first serious attempt at a comprehensive analysis of all coupling and other effects associated with median plane motion in cyclotrons. Unfortunately, their analysis is based on a nonrelativistic Hamiltonian and formulated in Cartesian coordinates, and both of these premises impose rather severe restrictions on the scope and accuracy of their results.

Nevertheless, their impressive work has clearly outlined at least two important aspects of the coupling process which deserve further exploration. One of these concerns the proper definition of the phase  $\phi$  for particles executing radial oscillations about an equilibrium orbit. The second, related effect concerns a phase dependent shift in  $\nu_r$ , produced by the acceleration process which can, in certain cases, lead to radial instability.

Regarding the phase definition, one has, on the one hand, the phase  $\phi$  which determines the energy gained by a group of particles when averaged over many gap crossings and, on the other hand, the "local" phase ( $\omega_{rf}t$ ) which specifies the time at which different members of the group cross a particular gap. The problem of correlating these phases was solved, at least for a nearly

\* Work supported by the National Science Foundation under Grant No. Phy 78-22696

uniform magnetic field, by Schulte and Hagedoorn who identified  $\phi$  with a "central position phase."

This problem is reconsidered in Sec. 2 below where we show, more generally, that an appropriate definition for  $\phi$  can be obtained for particles executing radial oscillations simply by requiring that  $\phi$  be a constant of the motion for non-accelerated orbits, at least to first order. In this case, particles having the same  $\phi$  value will generally start out with different values for the local phase, but will finally end up with the same energy gain as if they had all been moving continuously in equilibrium orbits.

The other coupling phenomenon noted above, namely, the phase dependent effect of the acceleration process on the radial oscillations, was first examined by Bolduc and Mackenzie<sup>4</sup> in connection with some design calculations on the TRIUMF cyclotron. These investigators interpreted the phenomenon correctly, and showed that the distortion of the radial phase space area observed in their orbit computations could be accounted for, at least qualitatively, by a simple theoretical model.

In re-analyzing this problem, Schulte and Hagedoorn<sup>5</sup> showed that the results could be interpreted as a loss of radial stability near  $\nu_r = 1$  through a mechanism somewhat similar to the production of a stop-band at a half-integral resonance. In addition, they have pointed out that similar difficulties can be expected to occur in many other cyclotrons operating on high harmonics.<sup>6</sup>

Most of the present paper is devoted to this phenomenon, which we shall call "radial electric focusing." This name seems quite appropriate since, as we shall show, there is a striking similarity between the results obtained for this effect and those obtained in a previous paper dealing with vertical electric focusing.<sup>7</sup> This similarity even extends to the presence of alternating gradient focusing in both cases for certain dee geometries.

Indeed, we find here a kind of "complementarity" relationship between the radial and vertical electric focusing which resembles, at least on the surface, the one discovered by Dutto and Craddock<sup>8</sup> for a completely different aspect of electric focusing.

The relationship found here is especially surprising since the nature of the focusing force for the radial oscillations is basically so different from that for the vertical oscillations. In the radial

case, the force resembles an inertial force since it arises from the accelerated motion of the "reference frame." That is, the radial oscillations are performed about an equilibrium orbit which shifts outward in position at each gap crossing, and this outward shift has two components. The first consists of an average shift which is independent of the radial oscillations, while the second depends on the value of  $p_x/p$  for the particle crossing the gap. It is this latter component which is responsible for the radial focusing effect.

In retrospect, it now seems quite likely that this radial electric focusing played an important role in the successful operation of the "phase selection slits" developed by Blosser,<sup>9</sup> which were instrumental in providing single turn extraction and high quality external beams from the old MSU 50 MeV cyclotron.

## 2. DEFINITION OF THE PHASE $\phi$

We begin by considering particles of constant energy  $E$  performing radial oscillations about an equilibrium orbit which, for simplicity, is assumed to be a circle of radius  $R$ . If  $x = r - R$  is the radial displacement, then the conjugate momentum  $p_x$  is given by

$$p_x = (p/R) (dx/d\theta), \quad (1)$$

where  $p$  is the total momentum.

The variation of  $p_x$  is determined by the equation of motion

$$dp_x/d\theta = -pv_r^2x/R, \quad (2)$$

where  $\nu_r$  is the radial tune. If this equation is combined with (1) above, we find

$$(d^2x/d\theta^2) + \nu_r^2x = 0, \quad (3)$$

which is the standard form.

We next consider how  $t$  varies with  $\theta$  for the oscillating particles. Here, the path length element is given by  $ds = vdt = rd\theta$ , to first order, from which we obtain

$$dt/d\theta = r/v = (R + x)/R\omega, \quad (4)$$

where, as usual,  $\omega = v/R$ .

Combining this expression with (2) above, we then find

$$\frac{d}{d\theta} (\omega t - \theta + p_x/pv_r^2) = 0, \quad (5)$$

from which it follows that the quantity in parenthesis is a constant of the motion, at least to first order.

The cyclotron rf system is characterized by a fixed frequency  $\omega_{rf}$ , and if the machine is to operate properly, there must be a subharmonic  $\omega_0$  which closely matches the orbital frequency  $\omega$ ; that is,

$$\omega_{rf}/h = \omega_0 \approx \omega, \quad (6)$$

where  $h$  is the harmonic number. We shall assume for simplicity that  $\omega = \omega_0$  at all energies, since deviations from this isochronism condition (which are normally quite small) need not concern us here.

When treating only the longitudinal motion in cyclotrons, it is customary to define the phase  $\phi$  (aside from some additive constant) by

$$\phi = \langle \omega_{rf}t - h\theta \rangle, \quad (7)$$

where the angular brackets indicate an average taken over the radial oscillations, or over many gap crossings. Under these average conditions, the particles can be considered as moving continuously in equilibrium orbits, and the energy gain per turn can then be taken as

$$\Delta T = \oint q\mathbf{E} \cdot d\mathbf{s} = qV_1 \cos \phi, \quad (8)$$

where the integration is around the closed equilibrium orbit, and  $V_1$  is the peak voltage gain per turn. We shall use  $T$  specifically for the energy of a particle moving in an equilibrium orbit.

When dealing with the coupling between the radial and longitudinal motion, it proves more useful to extend the definition of  $\phi$  so as to include the radial oscillations. To do this, we make use of (5) and set

$$\phi = \omega_{rf}t - h\theta + hp_x/pv_r^2, \quad (9)$$

which, since  $\omega_{rf} = h\omega$  here, is a constant of the motion, and which, moreover, reduces to the definition (7) above on the average.

This revised definition of  $\phi$  differs somewhat from that of the "central position" phase used by Schulte and Hagedoorn,<sup>3</sup> but the basic ideas are essentially the same. The advantage of revising the phase definition is illustrated in Fig. 1 in the simple case of a uniform magnetic field, where the two definitions coincide.

Since the extra term in (9) is proportional to both  $h$  and  $p_x/p$ , its effect will be most important

in the central region, and especially so for high harmonics.

Consider now a group of orbits starting at some point in the machine with exactly the same energy, and suppose that this group covers an eigenellipse in the  $(x, p_x)$  plane centered on the equilibrium orbit, or some other appropriate central ray. The approximately invariant area of this ellipse determines the final emittance corresponding to this group.

Thus, the initial state is completely specified except for the values of  $\omega_{rf}t$  at the given  $\theta$  value. It should now be recognized that, for the sake of consistency, these orbits should all be assigned the same value of  $\phi$ , as defined in (7). We should therefore use

$$\omega_{rf}t = h\theta + \phi - hp_x/pv_r^2, \quad (10)$$

to determine the "local phase"  $\omega_{rf}t$  for each member of the group.

If these orbits are now accelerated to extraction, it will then be found that they all end up with very nearly the same final energy since, according to (8), they all experience the same energy gain per turn on the average. Thus, the energy homogeneity is nearly invariant, and this is a very desirable property for groups of orbits characterizing the extracted beam.

We can, of course, pursue this argument all the way back to the ion source or injector. We must then conclude that energy homogeneity requires that different members of the group start out at different initial times.

These arguments apply most particularly to cyclotrons designed to operate with single turn extraction. When multiturn extraction is being investigated, the extension of this viewpoint requires that each  $\phi$  value be represented by a separate group of orbits.

Before proceeding, it seems appropriate to comment briefly on canonical variables because of their importance in phase space dynamics. One usually learns that in addition to  $r$  and  $p_r$ ,  $t$  and  $p_t = -E$  are canonically conjugate variables.

It turns out, however, that the transformation which changes from  $r$  and  $p_r$  to  $x$  and  $p_x$  also changes the variable conjugate to  $E$  from  $t$  to  $\phi/\omega_{rf}$ , where this  $\phi$  is the same phase as defined in (9) above.

Although this definition for  $\phi$  is rigorously correct only for circular equilibrium orbits, it should nevertheless be reasonably accurate for most cyclotrons. A more general definition will not be

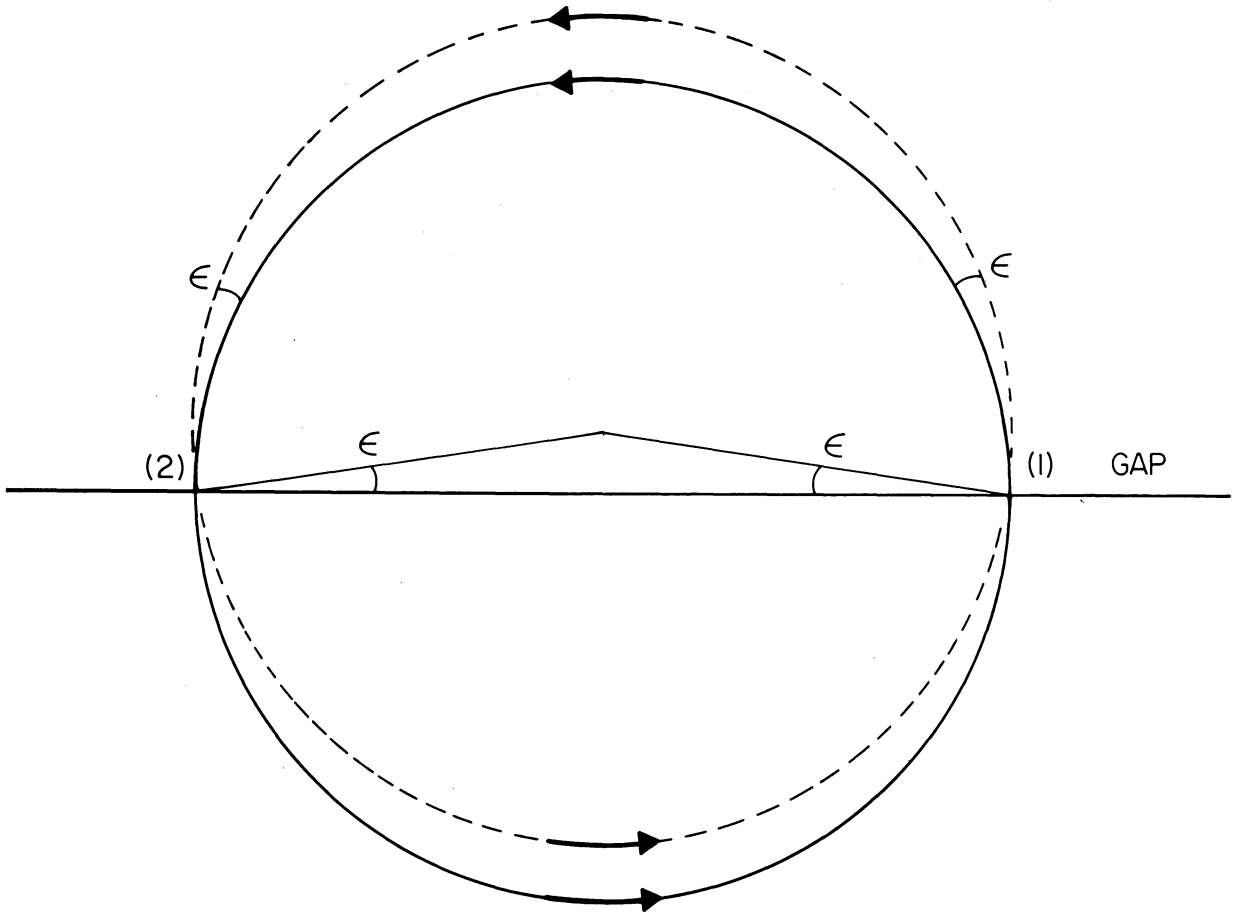


FIGURE 1 Phase Definition for Circular Orbits in a Uniform Magnetic Field. Horizontal line represents voltage gap which ions cross at (1)  $\theta = 0$  and (2)  $\theta = \pi$ . The rf voltage frequency is  $\omega_{rf} = h\omega$ , with  $h$  an odd integer. For an ion moving in the equilibrium orbit (solid circle), the voltage phase changes by  $h\pi$  during the ion's transit both from (1) to (2) and from (2) to (1). Thus, the ion gains the same energy at both crossings,  $qV_0 \cos \phi$ , where  $\phi = h\omega t_0$  if  $t_0$  is the ion's arrival time at (1), assuming the voltage peaks at  $t = 0$ . The ion moving in the displaced orbit (broken circle) crosses the gap moving outward from the equilibrium orbit at an angle  $p_x/p = +\epsilon$  at (1), and  $p_x/p = -\epsilon$  at (2). Here, the voltage phase changes by  $h(\pi + 2\epsilon)$  during the ion's transit from (1) to (2), and by

$h(\pi - 2\epsilon)$  during the transit back to (1). If this ion is to gain the same energy on the average (to first order in  $\epsilon$ ), then it must cross at (1) at the earlier time  $t_1 = t_0 - \epsilon/\omega$ , where it therefore gains  $qV_0 \cos(\phi - h\epsilon)$ , and it will then gain  $qV_0 \cos(\phi + h\epsilon)$  when it crosses at (2). Hence, the average energy gain per turn is  $2qV_0 \cos \phi$ , independent of  $\epsilon$ , to first order. Note that the ion in the displaced orbit experiences what amounts to a voltage asymmetry in the two gap crossings, and this will produce movement of its orbit center parallel to the gap. For  $\phi > 0$ , it moves to the left, while for  $\phi < 0$ , it moves to the right. In either case, this motion will produce a stretching of the radial phase space area, as discussed in Sec. 7.

presented here since the added mathematical complexity tends to obscure the nature of the phenomena.

### 3. GAP CROSSING EFFECTS

Consider the orbit of a particle which, during one particular gap crossing, acquires an energy gain  $\delta E$ . The corresponding equilibrium orbit shifts

outward by an amount  $\delta R$  given by

$$\begin{aligned} \delta R &= (dR/dp)(dp/dE)\delta E \\ &= R(\delta E)/v p v_r^2, \end{aligned} \quad (11)$$

as follows from  $dE = v dp$ , and the smooth-approximation formula for  $dp/dR$ .

Assuming, as is usual, that the angular width of the gap is negligibly small, then the value of

$r$  for the orbit under consideration remains essentially unchanged. Since  $r = R + x$  for this orbit, then as a result of the gap crossing, the value of  $x$  changes by

$$\delta x = -\delta R = -R(\delta E)/v p v_r^2, \quad (12)$$

which can be interpreted as providing a boundary condition on the radial oscillations executed by the particle.

For the purposes of the present discussion, it will be assumed that this is the only boundary condition resulting from the gap crossing. That is, we shall neglect possible changes in  $p_x$  which are produced, for example, by spiral electric gaps since the effects of such changes have already been considered elsewhere.<sup>10</sup>

For convenience, we use (2) to define a quantity  $F_x$  resembling the "restoring force"

$$F_x = -p v_r^2 x / R = d p_x / d \theta, \quad (13)$$

so that the boundary condition (12) is equivalent to a change in this force by an amount

$$\delta F_x = -p v_r^2 (\delta x) / R = (\delta E) / v. \quad (14)$$

Finally, this reduces to  $\delta F_x = \delta p$ , which might have been anticipated.

The value of  $\delta E$  at the particular gap crossing under consideration depends on the local phase  $\omega_{rf} t$ , and hence, from (10), on the value of  $p_x$  as well as  $\phi$ . If  $\delta T$  denotes the corresponding energy gain for a particle in the equilibrium orbit, we then have by series expansion

$$\delta E = \delta T - (h p_x / p v_r^2) \frac{\partial}{\partial \phi} (\delta T), \quad (15)$$

to first order in  $p_x/p$ . Thus,  $\delta F_x$  in (14) separates into two distinct terms.

The first of these,  $\delta F_x = \delta T/v$ , is independent of  $x$  and  $p_x$ , and therefore introduces an inhomogeneous term into the differential equation for the linear oscillations. Such a term has the effect of producing a quasi-periodic displacement of the equilibrium orbit. This displaced orbit is sometimes called the "accelerated equilibrium orbit" and its properties are fairly well known.<sup>3,10</sup> We shall therefore omit this term from now on, since it has no direct influence on our subsequent discussion.

The second term in  $\delta E$  above, and hence in  $\delta F_x$  of (14), is proportional to  $p_x$ , and therefore acts to modify the form and frequency of the linear

oscillations. This term can be rewritten

$$\frac{\delta F_x}{p_x} = - \left( \frac{h}{2 T_c v_r^2} \right) \frac{\partial}{\partial \phi} (\delta T), \quad (16)$$

where we have set  $\frac{1}{2} v p = T_c$ , the (non-relativistic) kinetic energy evaluated at the center of the gap. It is the effect of this boundary condition by itself that we shall consider here since it is this effect which appears both novel and interesting.

Before proceeding, we should note that in accordance with (12), this boundary condition is equivalent to<sup>14</sup>

$$\delta x = \frac{h R}{2 T_c v_r^4} \left( \frac{p_x}{p} \right) \frac{\partial}{\partial \phi} (\delta T). \quad (17)$$

Hence, since this  $\delta x$  is proportional to  $p_x/p$ , the effect on the radial oscillations is somewhat similar to that obtained by adding a set of straight sections to a synchrotron ring, for example.

#### 4. RADIAL ELECTRIC FOCUSING

In a recent paper<sup>7</sup> dealing with electric focusing, we considered a fairly general dee geometry and derived a formula for the resultant  $\delta T$  vs.  $\phi$  at each gap crossing. The same formula will be used here, and a brief review of the physical situation therefore seems in order.

The assumed geometry contains a set of  $N_d$  identical dees which are symmetrically arranged and uniformly separated in azimuth so that

$$\Delta \theta = \theta_e = 2\pi / N_d, \quad (18)$$

constitutes an electric "sector." In each of these sectors, the ions undergo one gap crossing when they enter the dee and another when they exit. Each dee is assumed to have a constant angular width  $D$ , so that

$$\theta_2 - \theta_1 = D < \theta_e, \quad (19)$$

where  $\theta_1$  and  $\theta_2$  are the angles where the ions enter and exit the dee, respectively.

An example of this situation is shown schematically in Fig. 2, and the voltage curves given there should help in understanding the energy gain formula given below.

As previously shown, the energy gain at  $\theta_1$  and  $\theta_2$  is given by

$$\delta T_j = q V_0 \sin(\frac{1}{2} h D + (-1)^j \phi), \quad (20)$$

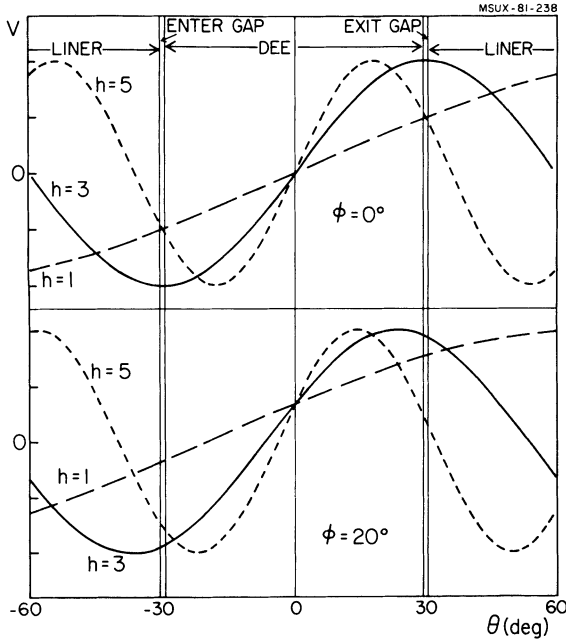


FIGURE 2 Energy gain versus phase  $\phi$  for different harmonics  $h$  and for dees having an angular width  $D = 60^\circ$ , like those in the MSU superconducting cyclotron. Here, the ions cross the first gap on entering the dee at  $\theta = -30^\circ$ , and the second gap on exiting the dee at  $\theta = +30^\circ$ . If the dee voltage (relative to the liner) is  $V_0 \sin \omega_r t$ , then,  $V_0 \sin(h\theta + \phi)$  is the value as seen by an ion having the phase  $\phi$  which, in this geometry, is given by  $\phi = \omega_r t - h\theta$ . Curves for this voltage are shown for  $\phi = 0^\circ$  (top) and  $\phi = 20^\circ$  (bottom), for the harmonics  $h = 1$  (long dashes),  $h = 3$  (solid line), and  $h = 5$  (short dashes). Here, the ion's energy gain on entering the dee is  $-qV_0 \sin(h(-30^\circ) + \phi) = qV_0 \sin(h(30^\circ) - \phi)$ , and on exiting, it is:  $qV_0 \sin(h(30^\circ) + \phi)$ , in accord with Eq. (20). The sum of these two gains is  $2qV_0 \sin(h(30^\circ)) \cos \phi$ , as in Eq. (21).

where  $j = 1$  or  $2$ , and  $V_0$  is the nominal dee voltage. As a consequence, the total energy gain per turn, obtained by summing over all  $2N_d$  gaps, is found to be

$$\Delta T = 2N_d q V_0 \sin(hD/2) \cos \phi, \quad (21)$$

which agrees in form (as it should) with the defining equation (8), and thereby provides the value of  $V_1$ .

The above  $\delta T_j$  can now be used to calculate the derivative in (16), namely,

$$\begin{aligned} \frac{\partial}{\partial \phi} (\delta T_j) &= -qV_0 \sin(hD/2) \sin \phi \\ &+ (-1)^j qV_0 \cos(hD/2) \cos \phi. \end{aligned} \quad (22)$$

Here again, the voltage curves in Fig. 2 should help in understanding the result.

Again letting  $T$  denote the kinetic energy (for a particle in the equilibrium orbit), we introduce a dimensionless energy variable  $n_0$  defined by

$$n_0 = T/qV_1, \quad (23)$$

and a comparison with (8) above shows that  $n_0$  is the turn number for  $\phi = 0$ .

Making use of this definition, the boundary condition (16) at the two gap crossings now becomes

$$\begin{aligned} \alpha_j &= \frac{\delta F_x}{p_x} = \frac{+h}{4n_0 N_d v_r^2} \\ &\times (\sin \phi - (-1)^j \cot(hD/2) \cos \phi), \end{aligned} \quad (24)$$

which also serves to define  $\alpha_j$ . Although  $n_0$  is different at each gap, this difference will be neglected for simplicity, at least in the analytical calculations.

As will be shown, the first term here leads to ordinary focusing, while the second term produces AG focusing since it alternates in sign. Evidently, these effects are most important for low turn numbers and high harmonics.

For reasons which will become clear later, we now change variables from  $x$  to  $p_x$  in describing the linear oscillations. Thus, Eqs. (1, 2) can be combined to yield

$$(d^2 p_x / d\theta^2) + v_r^2 p_x = 0, \quad (25)$$

which now becomes the equation of motion between gap crossings, thereby replacing (3) for  $x$ .

The solution of this equation is subject to the boundary conditions at each gap crossing, and within each electric sector, these conditions now become

$$\delta F_x = \delta(dp_x/d\theta) = \alpha_j p_x, \quad (26)$$

in accordance with Eqs. (13, 24) above.

Solutions satisfying these conditions can be combined so as to generate the transfer matrix for the complete sector (18). The effect of the perturbation can then be expressed directly in terms of a revised focusing frequency, which we shall call  $v_r^*$ .

When this process is carried through, the result

is

$$\begin{aligned} \cos(\nu_r^* \theta_e) &= \cos \nu_r \theta_e \\ &+ \left( \frac{\alpha_1 + \alpha_2}{2\nu_r} \right) \sin \nu_r \theta_e \\ &+ \left( \frac{\alpha_1 \alpha_2}{2\nu_r^2} \right) \sin \nu_r (\theta_e - D) \sin \nu_r D. \end{aligned} \quad (27)$$

Note that the term containing  $(\alpha_1 + \alpha_2)$  corresponds to ordinary focusing, while the term containing  $\alpha_1 \alpha_2$  produces AG focusing.

To be more specific, we consider cyclotrons having two dees, which cover a wide variety of designs including the TRIUMF cyclotron with  $D = 180^\circ$  and the Indiana cyclotron with  $D = 38^\circ$ . For such machines,  $N_d = 2$  and  $\theta_e = \pi$ , so that the above formulas yield

$$\begin{aligned} \cos \pi \nu_r^* &= \cos \pi \nu_r + \left( \frac{h \sin \phi}{8n_0 \nu_r^3} \right) \sin \pi \nu_r \\ &- \frac{1}{2} \left( \frac{h}{8n_0 \nu_r^3} \right)^2 (\cot^2(hD/2) \cos^2 \phi \\ &- \sin^2 \phi) \sin \nu_r (\pi - D) \sin \nu_r D. \end{aligned} \quad (28)$$

This case is probably the most interesting because  $\nu_r \approx 1$  near the center of most cyclotrons. Thus, as a result of the added electric focusing, the radial oscillations may become unstable through the creation of a stop-band wherein  $(\nu_r^* - 1)$  becomes imaginary, that is,  $|\cos \nu_r^* \theta_e|$  exceeds unity.

To see this more clearly, we set  $\nu_r = 1$  and  $\phi = 0$  in the above formula, and thereby obtain

$$\begin{aligned} \cos \pi(\nu_r^* - 1) &= 1 + \frac{1}{2}(h/8n_0)^2 \\ &\times \cot^2(hD/2) \sin^2 D. \end{aligned} \quad (29)$$

Here,  $(\nu_r^* - 1)$  is obviously imaginary for all conditions except where  $D = 180^\circ$  or  $\cos(hD/2) = 0$ .

Another situation of special interest, mainly because of its simplicity, is the limit where the electric focusing becomes very weak. That is, for small values of  $h/n_0$ , we can set  $\nu_r^* = \nu_r + \Delta\nu_r$ , and calculate  $\Delta\nu_r$  by a simple expansion. In this

case, Eqs. (27, 24) yield

$$\begin{aligned} \Delta\nu_r^2 &= -(\alpha_1 + \alpha_2)/\theta_e \\ &= -\frac{h \sin \phi}{4\pi n_0 \nu_r^2}, \end{aligned} \quad (30)$$

where  $\Delta\nu_r^2 = 2\nu_r \Delta\nu_r$ . This result is evidently the same for all dee geometries since it is independent of the parameters  $N_d$  and  $D$ .

## 5. FOCUSING COMPLEMENTARITY

Before applying the foregoing analysis to specific cyclotrons, we digress here to compare the results with those obtained in a previous paper dealing with vertical electric focusing.<sup>7</sup> Surprisingly enough, the two analyses parallel each other very closely.

Indeed, almost every equation in the preceding section on radial electric focusing has an exact analog in a corresponding equation for vertical electric focusing given in our previous paper. To transform one set of results into the other, we need only to replace  $p_x$  by  $z$ ,  $\nu_r$  by  $\nu_z$ , and  $\alpha_j$  by  $\beta_j$ .

The replacement of  $\alpha_j$  by  $\beta_j$  corresponds simply to a change in the boundary condition at the gaps, and the nature of this change is perhaps the most remarkable of all. To show this, we present these boundary conditions again for direct comparison

$$\alpha_j = \frac{\delta(dp_x/d\theta)}{p_x} = \frac{-h}{2T_c \nu_r^2} \frac{\partial}{\partial \phi} (\delta T_j), \quad (31a)$$

$$\beta_j = \frac{\delta(dz/d\theta)}{z} = \frac{+h}{2T_c} \frac{\partial}{\partial \phi} (\delta T_j), \quad (31b)$$

where  $\alpha_j$  comes from Eqs. (24, 16) above, and  $\beta_j$  comes from analogous equations in our previous paper.

Evidently, these focusing parameters are related by

$$\beta_j + \nu_r^2 \alpha_j = 0, \quad (32)$$

and such a relationship signifies a kind of "complementarity" between the radial and vertical electric focusing, such that any acceleration condition which increases one must necessarily decrease the other.

To make this complementarity more evident,

consider the special case where the focusing is weak. In this limit, we find

$$\Delta v_z^2 = \frac{+h \sin \phi}{4\pi n_0}, \quad (33)$$

according to the result given in our previous paper<sup>7</sup> (where  $n_0$  was denoted by  $n$ ). This formula is directly comparable in its applicability to the one given for  $\Delta v_r^2$  in Eq. (30) above. Combining the two results, we obtain

$$\Delta v_z^2 + v_r^2 \Delta v_r^2 = 0, \quad (34)$$

which exemplifies the relationship.

This complementarity is distinct from and supplementary to the one discovered by Dutto and Craddock<sup>8</sup> in connection with modifications of the electrode structures defining the gaps. Specifically, they showed that when the electric field is deformed so as to increase the vertical focusing, it simultaneously decreases the radial focusing in accordance with

$$\Delta v_z^2 + \Delta v_r^2 = 0. \quad (35)$$

Moreover, since  $v_r \approx 1$  in the central region where these focusing effects are most important, the similarity between this result and Eq. (34) above becomes even more evident.

This focusing complementarity is reminiscent of a similar relationship for magnetic focusing where a change in the average field index  $\Delta k$  leads to focusing changes

$$\Delta v_r^2 = \Delta k = -\Delta v_z^2. \quad (36)$$

It is also very reminiscent of the "incompatibility" between radial and longitudinal focusing in linear accelerators which, when viewed in the reference frame of the moving ions where the electric field becomes static, can be explained by Earnshaw's theorem of electrostatics.<sup>11</sup>

## 6. EXAMPLES

We consider first cyclotrons having just two gap crossings per turn, corresponding to 180° dees. This case concerns a large number of the cyclotrons now in operation, since it includes those having a single dee, as well as those having two 180° dees operating in push-pull. Among the former, we should note in particular the VEC machine at Harwell<sup>12</sup> which has operated for a long

time now on harmonics up to  $h = 9$ , and among the latter, the TRIUMF cyclotron, which will be discussed in the next section.

The  $v_r^*$  formula for all these machines can be obtained simply by setting  $D = \pi$  in Eq. (28), so that

$$\cos \pi v_r^* = \cos \pi v_r + \left( \frac{h \sin \phi}{8n_0 v_r^3} \right) \sin \pi v_r, \quad (37)$$

where  $n_0 = T/2qV_0$  as follows from (23). For comparison, the corresponding expression for  $v_z^*$  is

$$\cos \pi v_z^* = \cos \pi v_z - \left( \frac{h \sin \phi}{8n_0 v_z} \right) \sin \pi v_z, \quad (38)$$

as follows, for instance, from the discussion in the preceding section. Note the similarity in the two formulas including the absence of AG focusing from both.

Since  $(v_r - 1)$  is quite small in the central region, it proves useful to expand (37), so that

$$(v_r^* - 1)^2 = (v_r - 1)^2 - \left( \frac{h \sin \phi}{4\pi n_0} \right) (v_r - 1), \quad (39)$$

to first order. Generally speaking,  $v_z$  is also small in the central region, and a corresponding expansion of (38) yields

$$(v_z^*)^2 = v_z^2 + \frac{h \sin \phi}{4\pi n_0}, \quad (40)$$

again to first order. This result corresponds exactly to (33) above.

Since the primary problem is securing sufficient vertical focusing, the source-puller geometry is usually designed so as to inject the beam with  $\phi > 0$ . As can be seen from (40), this procedure increases  $v_z$ , but at the same time, (39) shows that it may cause the radial oscillations to become unstable. That is,  $(v_r^* - 1)$  will be imaginary, and a stop-band will therefore exist, for values of the energy  $T$  such that

$$\frac{qV_0 h \sin \phi}{2\pi T} (v_r - 1) > (v_r - 1)^2. \quad (41)$$

It is the potentially harmful effects of this instability, especially for high harmonics, which have been emphasized by Schulte and Hagedoorn.<sup>6</sup>



This instability may, however, turn out to be less dangerous than anticipated. First, it should be recognized that the product  $h \sin \phi$  occurs in all formulas above. Thus, when  $h$  needs to be increased, then  $\sin \phi$  can be decreased accordingly, so that the vertical as well as the radial focusing remain unchanged.

Second, most cyclotrons have a central magnet "cone" which, for the first few turns at least, supplies some magnetic focusing and, simultaneously, keeps  $\nu_r$  below unity. In this case,  $(\nu_r - 1)$  is negative, and (39) shows that no instability will therefore be produced when  $\phi > 0$ .

Moreover, when  $\nu_r$  passes through  $\nu_r = 1$  in these machines, it usually rises quite rapidly as a result of the concurrent rise in the flutter field. This rapid rise will also tend to mitigate the effect of the instability by shortening its duration.

As another, quite different example, we consider the low energy cyclotron ring at Indiana since, as previously reported,<sup>7</sup> this machine possesses unusual electric focusing characteristics. This cyclotron has two dees with  $D = 38^\circ$ , so that  $\nu_r^*$  can be calculated from Eq. (28), including the AG focusing terms.

Calculations based on field measurements indicate that the minimum  $\nu_r = 1.16$  occurs at the injection energy.<sup>13</sup> As shown in our previous paper, this energy corresponds roughly to turn  $n_0 = 4$ , as defined in (23).

Of all the harmonics which this cyclotron is designed to use, the  $\nu_r^*$  formula (28) indicates that AG focusing will be most significant for  $h = 8, 11$ , and  $17$ . Assuming  $\phi = 0$ , we find for both  $h = 8$  and  $17$ , that  $\nu_r^* = 1.15$ , an almost insignificant change from its original value,  $\nu_r = 1.16$ .

If we assume  $\phi = +30^\circ$ , a rather extreme value, we find  $\nu_r^* = 1.13$  for  $h = 8$ , and  $\nu_r^* = 1.08$  for  $h = 17$ . Thus, a change in  $\nu_r$  might be detected if the injection phase were shifted far enough, but under ordinary circumstances the effect would be negligible.

The absence of any instability in this case can be attributed to two factors. First, the injection energy (and hence  $n_0$ ) is relatively large, and second, as a result of the exceptionally high flutter, the value of  $(\nu_r - 1)$  is also unusually large. Both of these favorable factors are generally characteristic of separated sector cyclotrons, such as those at Indiana, and the effects of radial electric focusing should therefore be less significant for these machines.

## 7. TRIUMF CYCLOTRON

As a final example, we consider the central region of the TRIUMF cyclotron mainly because the orbit properties provide a good illustration of the theory. We should emphasize first that these orbit properties were studied very thoroughly by the original design group so that our analysis is aimed only at a re-interpretation of various phenomena discovered by these investigators.<sup>14</sup>

This truly unique cyclotron accelerates  $H^-$  ions to 520 MeV with a peak voltage gain per turn  $V_1 = 340$  kV, using an rf system operating on the harmonic  $h = 5$  of the relatively low orbital frequency (4.6 MHz) required for this machine. The  $H^-$  ions are injected with 300 keV energy, and finally extracted simply by stripping which makes possible the effective use of a relatively large phase width,  $45^\circ$ .

Since we are concerned here only with median plane motion, we have simplified all of the analytical calculations by assuming that the magnetic field is axially symmetric as well as perfectly isochronous, so that

$$B_z = B_0 [1 - (r\omega/c)^2]^{-1/2}, \quad (42)$$

where  $\omega = qB_0/m_0 = 2\pi(4.6 \text{ MHz})$ , corresponding to  $B_0 = 3.0$  kG. For this field, we have simply

$$\nu_r = \gamma = 1 + T/m_0c^2, \quad (43)$$

which can therefore be evaluated exactly.

In the energy region of interest here, Eq. (39) for  $\nu_r^*$  serves very well, and yields

$$(\nu_r^* - 1)^2 = (T/m_0c^2)^2 - (h/4\pi)(qV_1/m_0c^2) \sin \phi, \quad (44)$$

with the aid of (43). This equation shows that for  $\phi > 0$ , the radial oscillations will be unstable for values of  $T$  below some critical value

$$T_{\text{crit}} = (hqV_1m_0c^2 \sin \phi/4\pi)^{1/2}. \quad (45)$$

Using  $\phi = 22.5^\circ$  and the data given above, we obtain  $T_{\text{crit}} = 6.8$  MeV, which corresponds to about 20 turns. Since the beam has a phase width of about  $45^\circ$ , this instability should be quite important here, as pointed out by Schulte and Hagedoorn.<sup>5</sup>

In describing the radial oscillations, it proves

useful to replace  $(x, p_x)$  by  $(\xi, \eta)$  defined by

$$\xi = \gamma \delta x, \quad \eta = \delta p_x / \gamma m_0 \omega, \quad (46)$$

where  $\delta x$  and  $\delta p_x$  represent deviations from some central ray orbit. In terms of these variables, the phase space eigenellipse reduces to a circle

$$\xi^2 + \eta^2 = \rho^2, \quad (47)$$

and moreover, the area  $\pi \rho^2$  is the corresponding action integral and therefore adiabatically invariant.

Thus, as long as the acceleration process is adiabatic, the  $(\xi, \eta)$  points corresponding to a particular orbit simply move clockwise around a circle of radius  $\rho$  with an angular velocity  $\gamma \omega$ , in accordance with the equations of motion (1,2) and  $v_r = \gamma$ . That is, if we introduce the complex vector

$$\zeta = \xi + i\eta = \rho e^{i\psi}, \quad (48)$$

then  $\rho$  is constant, and

$$\psi = - \int \gamma d\theta. \quad (49)$$

Use of the variables  $(\xi, \eta)$  therefore makes it easy to recognize when the motion is non-adiabatic or nonlinear.

In order to test the theory, we followed a procedure similar to that of Bolduc and Mackenzie<sup>4</sup> and carried out two sets of calculations. One involved "exact" calculation of a set of orbits using standard numerical integration techniques, while the other involved calculation of the same set of orbits using a theoretical transfer matrix.

We should note first that the numerical integrations used  $r, p_r, t,$  and  $E$  as variables and, between gap crossings, the exact equations of motion for the magnetic field given in (42). Then, at each gap, the energy is increased simply by

$$\delta E = \pm q V_0 \cos(h\omega t), \quad (50)$$

with  $h = 5$  and  $q V_0 = 170$  keV here. The (+) and (-) signs are used, respectively, at  $\theta = 0$  and  $\theta = \pi$ , the assumed locations of the gaps. Finally, this program uses  $\xi, \eta,$  and  $\phi$  only for input and output purposes.

On the other hand, the transfer matrix program is formulated entirely in terms of  $\xi$  and  $\eta$  as variables, with  $\phi$  an input parameter. This program assumes that between gap crossings the change

in  $(\xi, \eta)$  is obtained from

$$\zeta(\theta_2) = \zeta(\theta_1) \exp(-i\gamma(\theta_2 - \theta_1)), \quad (51)$$

in accordance with (48) above. Here,  $\phi$  is treated as a constant, as one would expect for an isochronous field, and the energy gain at each gap crossing is taken as

$$\delta T = q V_0 \cos \phi, \quad (52)$$

which is simply a constant.

In addition, the boundary condition on the point  $(\xi, \eta)$  at each gap is determined by the theoretical formula (17). This condition now becomes

$$\delta \xi = -\lambda \eta, \quad (53)$$

where  $\lambda$  is given by

$$\lambda = \frac{h q V_0 \sin \phi}{2 T_c \gamma^3}, \quad (54)$$

with  $h = 5$  and  $q V_0 = 170$  keV again. Here,  $T_c$  and  $\gamma$  are evaluated by using the average value of the energy before and after the gap crossing.

Before proceeding, we should point out that the above transfer matrix algorithm, when combined with a periodicity assumption, can be used to determine the revised form of the eigen-ellipse including the effect of the radial electric focusing. Such a procedure would parallel the one followed by Schulte and Hagedoorn,<sup>5</sup> and although our results are quite different from theirs, we shall omit the details here. Suffice it to say that the characteristic ellipse becomes a hyperbola within the stop-band, as one would expect.

However, this eigenellipse or hyperbola is quite irrelevant here since the elements of the transfer matrix change so rapidly with energy during the first twenty turns or so after injection. Under these highly non-adiabatic conditions, the transfer matrix itself provides much more significant information than can be obtained from  $v_r^*$  or the eigenellipse. That is, the transfer matrix program outlined above does not assume that the motion is adiabatic, but only that it is linear and that  $\phi$  is constant.

Returning now to our test of the theory, we next note that the coupling effects fall off with increasing energy as can be seen, for example, from the parameter  $\lambda$  in (54). It was therefore decided that, rather than starting at the injection

energy and running the orbits forward, we would instead run the orbits backward starting from a relatively high energy. Thus, the orbits start where the theory should be quite good, and as the energy decreases, the coupling effects become progressively stronger, and the resultant changes can then be examined systematically.

This procedure has another advantage in that we know beforehand what the ideal phase space distribution should be when the motion finally becomes adiabatic. That is, for high turn numbers, all particles with the same  $E$  and  $\phi$  should have  $(\xi, \eta)$  values which are compactly distributed within a small circle of radius  $\rho_0$  whose center point coincides with a perfectly centered orbit. Thus, if  $\rho_0$  is the same for all  $\phi$  values, the resultant beam would have the smallest possible emittance for the given current.

The orbit calculations to be described here were all started at 20 MeV, corresponding roughly to 60 turns beyond injection. Each set of orbit integrations consists of a central ray plus eight displaced rays.

In order to achieve perfect centering, the initial  $(r, p_r)$  for the central ray was empirically determined to match the accelerated equilibrium orbit mentioned in Sec. 3. In keeping with the above discussion, the initial  $(r, p_r)$  values for the eight displaced rays were so chosen that the corresponding  $(\xi, \eta)$  points were uniformly distributed on a circle of radius  $\rho_0$ .

The corresponding emittance for this set of orbits is given by

$$\oint dx dp_x/p = \pi \rho_0^2 / \gamma R, \quad (55)$$

since  $p = \gamma m_0 \omega R$  here. Values of  $\rho_0 = 2$  mm and 4 mm were both used, and these correspond, respectively, to emittances of  $12\pi$  and  $48\pi$  mm-mrad, when extrapolated back to injection ( $R = 0.33$  m).

Sets of runs were carried out for three different phase values:  $\phi = 0, +22.5^\circ$ , and  $-22.5^\circ$ , again following Bolduc and Mackenzie. It is important to remember that the orbit integration program uses  $\phi$  only for input and output, and for this purpose, it relates  $\phi$  to  $\omega_{rf}t$  and  $p_x/p$  through the basic definition in (9).

Figure 3 shows the evolution of the  $(\xi, \eta)$  phase space ellipse for  $\phi = +22.5^\circ$  and  $\phi = -22.5^\circ$  starting from turn  $n = 0$  (20 MeV) and going both backward to  $n = -60$  (1.1 MeV) and forward to  $n = +60$  (39 MeV). The solid ellipses were ob-

tained from the transfer matrix program and, as can be seen, the eight points from the orbit integrations all fall on the corresponding ellipses within the accuracy allowed by the plots, except at  $n = -60$ . These points all start at  $n = 0$  on a circle of radius  $\rho_0 = 4$  mm and the transformation of this circle into an ellipse with increasing eccentricity as  $n$  decreases signifies that the motion is becoming progressively more non-adiabatic.

The forward run to turn  $n = +60$  was carried out mainly to verify that the motion was essentially adiabatic beyond 20 MeV, the starting point. This verification is indicated in Fig. 3 which shows that the initial circle of points remains nearly circular (rather than becoming elliptical) at turn  $n = +60$ .

As the energy decreases in the backward runs down below about 2 MeV, the deviations of the computed points from the corresponding transfer matrix values increase very rapidly. Although the details will be omitted here, further investigation shows that these deviations are due partly to non-linear effects, and partly to energy differences between the central and displaced rays which our simple theory neglects. All the backward runs were terminated at 0.5 MeV where the theory evidently breaks down. In terms of the parameter  $n_0 = T/qV_1$  used in the theory, this energy corresponds to  $n_0 = 1.5$ , and we therefore conclude that the simple theory is reasonably good down to about  $n_0 = 3$ .

Figure 4 shows the results obtained when the plots of Fig. 3 are extended to 0.5 MeV, where the calculations stopped. In addition to the data for  $\phi = +22.5^\circ$  and  $-22.5^\circ$ , we include here results for  $\phi = 0$  which, by design, are also obtained at 0.5 MeV, but at turn  $n = -57$ .

The  $\phi = 0$  results were omitted from Fig. 3 since the computed points and ellipses do not deviate from their initial circles to any appreciable extent, as expected from the theory; that is,  $\lambda = 0$  for  $\phi = 0$ .

The most prominent feature of the curves shown in Fig. 3 and Fig. 4 is the "stretching" which appears proportional to  $\sin \phi$ , as in the parameter  $\lambda$  of (54). Although the stretching is greater for  $\phi = +22.5^\circ$  than for  $\phi = -22.5^\circ$ , the general similarity of the two cases can be understood qualitatively from the explanation given with Fig. 1.

To help in making the stretching mechanism somewhat clearer, we present Fig. 5 where, for

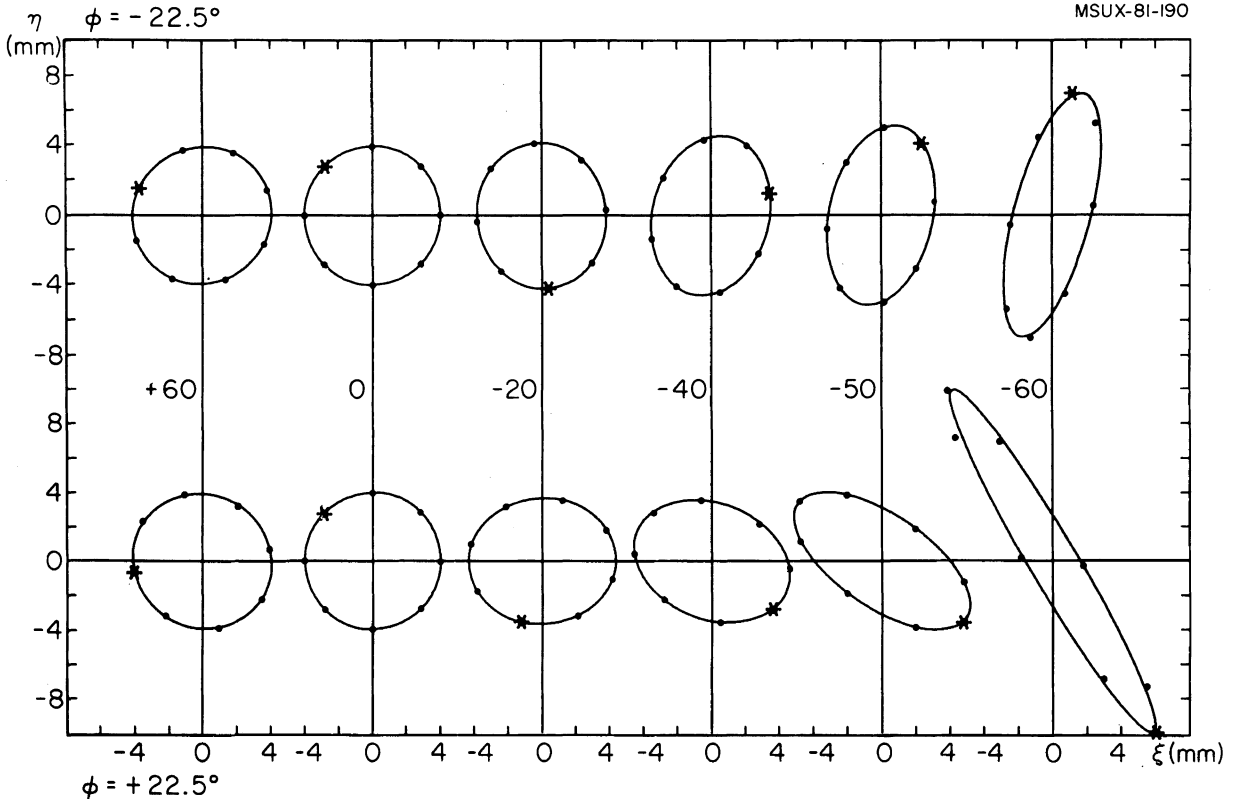


FIGURE 3 Evolution of radial phase space area for  $\phi = +22.5^\circ$  (bottom) and  $\phi = -22.5^\circ$  (top). Plots of  $\eta = \delta p_x / \gamma m_0 \omega$  versus  $\xi = \gamma \delta x$  made at  $\theta = 90^\circ$  (midway between gap crossings) from computer data obtained for orbits starting at turn  $n = 0$  (20 MeV), and running forward to  $n = +60$  (39 MeV), shown at far left, and then running backward to  $n = -20$  (14 MeV),  $n = -40$  (7.4 MeV),  $n = -50$  (4.3 MeV),

and  $n = -60$  (1.1 MeV), shown in sequence to the right. The eight plotted points are from "exact" orbit computations, while the solid ellipses are from a theoretical transfer matrix program. All calculations (including those for  $\phi = 0$ ) start from  $(\xi, \eta)$  points on a circle of radius  $\rho_0 = 4$  mm as shown here for  $n = 0$ . The "asterisks" mark the points for one particular orbit, which is used for reference.

each  $\phi$  value, plots of  $\eta$  versus  $\xi$  are given corresponding to the particular orbit indicated by the "asterisk" in Fig. 3 and Fig. 4. These  $(\xi, \eta)$  points are plotted regularly once every five turns, and the changes in the precession (rotation) rates are quite apparent.

These changes, and their dependence on  $\phi$ , can be accounted for by Eq. (44). For  $\phi = +22.5^\circ$ , in particular, this equation shows that  $(\nu_r^* - 1)$  goes to zero near turn  $n = -42$  where the energy is 6.8 MeV corresponding to the critical energy given in (45) above. That is, for  $n < -42$  in this case, the  $(\xi, \eta)$  points reverse direction and move outward at a rapidly increasing rate. This outward motion corresponds to the type of phase space behavior associated with the stop-band of a half-integral resonance.

The foregoing results show clearly why it is so difficult to match the radial emittance of the injected beam to the radial acceptance of the cyclotron over a large phase range. In TRIUMF, the beam is injected with 300 kV at  $\theta = 0$ , the center of a gap, and with a phase range, say, from  $\phi = 0$  to  $45^\circ$ . For a situation like this, the only simple rule seems to be that the injected beam should have an antifocus (i.e., be collimated) at the injection point ( $\theta = 0$ ) since this will minimize the radial electric defocusing.

Turning next to the results obtained for the phase and energy variations, we find, first of all, that the energy gain per turn for the central ray orbits themselves is remarkably constant, varying by less than 0.01 keV in all cases, thereby confirming Eq. (52) for  $\delta T$ . At the same time, the

value of  $\phi$  for these orbits varies by less than  $0.03^\circ$  while the value of  $hp_x/p$  in Eq. (9) rises to a maximum value of  $0.42 \text{ rad} = 24^\circ$  at the lowest energy,  $0.05 \text{ MeV}$ .

The energy and phase results for the displaced rays is more complicated, and only a brief summary will be given here. First, the expansion (15) for the energy gain at each gap crossing, when combined with Eq. (50) above, now becomes

$$\delta E = qV_0 \cos \phi + (h\eta/R\gamma^2)qV_0 \sin \phi, \quad (56)$$

with  $h = 5$  and  $qV_0 = 170 \text{ keV}$  here. Thus, the energy gain depends on  $\eta$ , and some of the effects of this dependence have been discussed by Schulte and Hagedoorn.<sup>3</sup> Our own results indicate that, in addition to the linear  $\eta$  term given above, the quadratic term is also necessary to explain the data satisfactorily.

Perhaps the most interesting feature of our numerical results is the remarkable constancy of the phase values. If we let  $\delta\phi = |\phi - \phi_c|$  be the magnitude of the difference between the phase values for the given orbit and for the corresponding central ray ( $\phi_c$ ), then, bearing in mind that  $\delta\phi = 0$  for  $n = 0$ , our results show that for the orbits described in Fig. 3,  $\delta\phi$  is less than  $0.025^\circ$  for turn numbers up to  $n = +60$  and down to  $n = -50$ . From  $n = -50$  to  $-60$ , the largest  $\delta\phi$  rises to  $0.15^\circ$ . These results (and other similar results) provide convincing evidence for the superiority and usefulness of the revised phase definition given in (9).

In conclusion, we should like to express our appreciation to D.A. Johnson who wrote the program used to carry out the exact orbit computations described above.

MSUX-8I-19I

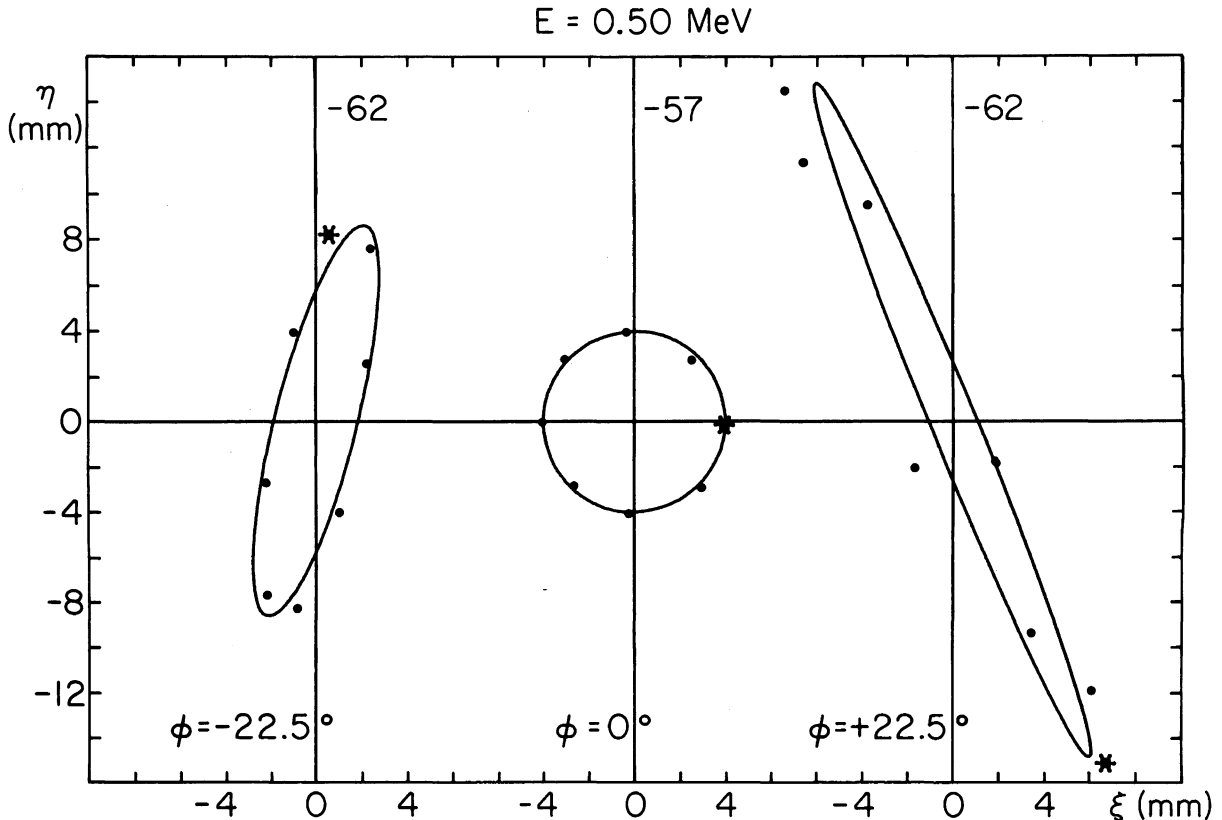


FIGURE 4 Continuation of the radial phase space plots displayed in Fig. 3 down to  $E = 0.5 \text{ MeV}$ , where all the computations were stopped. These plots show  $\eta$  versus  $\xi$  values

for  $\phi = -22.5^\circ$  (left),  $\phi = +22.5^\circ$  (right), both at turn  $n = -62$ , and for  $\phi = 0$  (center) at turn  $n = -57$ .

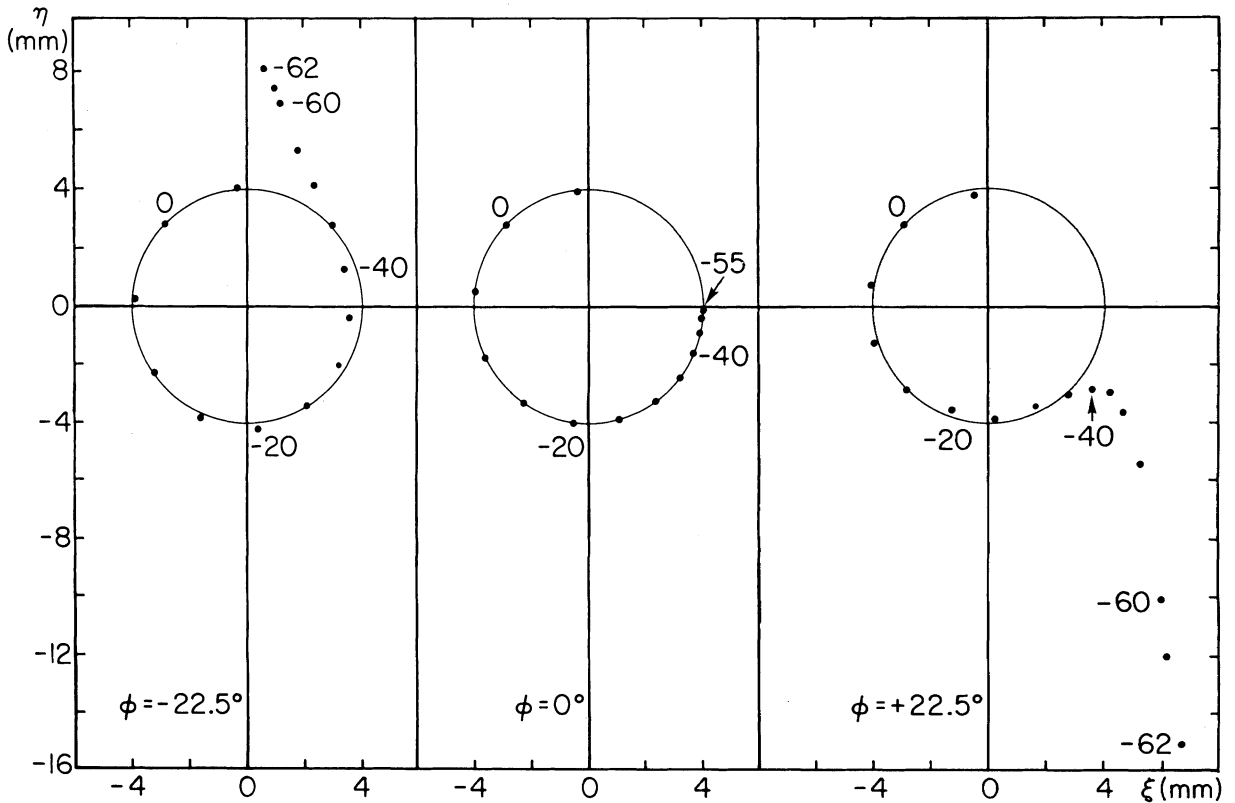


FIGURE 5 Radial phase space plots for the three particular orbits marked by asterisks in Fig. 3 and Fig. 4. Plots of  $(\xi, \eta)$  points for  $\phi = -22.5^\circ$  (left) and  $\phi = +22.5^\circ$  (right) go from  $n = +5$  down to  $n = -60$  with an interval  $\Delta n = 5$ , and then to  $n = -61$  and  $-62$  (0.5 MeV). At center, plot for  $\phi = 0$  orbit goes from  $n = +5$  down to  $n = -55$  with  $\Delta n$

$= 5$ , but points for  $n = -56$  and  $-57$  (0.5 MeV) are omitted since they practically coincide with the  $n = -55$  point. The solid curve is a circle of radius  $\rho_0 = 4$  mm shown for reference. The  $(\xi, \eta)$  points from  $n = +5$  to  $n = +60$  simply march around this circle and have been omitted here to avoid overplotting.

## REFERENCES

1. B. L. Cohen, *Rev. Sci. Instrum.* **24**, 589 (1953).
2. M. M. Gordon, *Nucl. Instrum. Methods* **18-19**, 268 (1962).
3. W. M. Schulte and H. L. Hagedoorn, *Nucl. Instrum. Methods* **171**, 409 (1980).
4. J. L. Bolduc and G. H. Mackenzie, *IEEE Trans. Nucl. Sci.* **NS-18**, 287 (1971).
5. W. M. Schulte and H. L. Hagedoorn, *Nucl. Instrum. Methods* **137**, 15 (1976).
6. W. M. Schulte and H. L. Hagedoorn, *IEEE Trans. Nucl. Sci.* **NS-26**, 2329 (1979).
7. M. M. Gordon and F. Marti, *Particle Accelerators* **11**, 161 (1980).
8. G. Dutto and M. K. Craddock, *Proc. 7th Int. Conf. on Cyclotrons and their Applications*, (Birkhauser, Basel, 1975) p. 271. G. Dutto and M. K. Craddock, TRIUMF Report TRI-DN-71-21 (1971).
9. H. G. Blosser, 5th Int. Cyclotron Conf., (Butterworths, London, 1971) p. 257.
10. M. M. Gordon, *Nucl. Instrum. Methods* **169**, 327 (1980).
11. A. A. Kolomensky and A. N. Lebedev, *Theory of Cyclic Accelerators* (North Holland, Amsterdam, 1966), ch 1.
12. E. J. Jones and K. J. Howard, 5th Int. Cyclotron Conf., (Butterworths, London, 1971) p. 318. J. A. Martin, *IEEE Trans. Nucl. Sci.* **NS-26**, 2554 (1979).
13. B. M. Bardin, J. H. Hettmer, W. P. Jones, and C. J. Kost, *IEEE Trans. Nucl. Sci.* **NS-18**, 311 (1971).
14. G. Dutto, C. Kost, G. H. Mackenzie, and M. K. Craddock, *Proc. 6th Int. Cyclotron Conf.* (AIP, New York, 1972) p. 340. E. W. Blackmore et al., *IEEE Trans. Nucl. Sci.* **NS-20**, 248 (1973).